GBT 26-40 GHz Radiometer

Design Considerations for the Continuum Section

S. Padin

California Institute of Technology

MS105-24 Pasadena CA 91125

22nd June 2001

I. Introduction

The 26-40 GHz receiver proposed for the GBT is a differential radiometer, similar to those built for the MAP satellite [1]. In its simplest form, this type of differential radiometer has a pair of amplifiers connected between two magic tees, as shown in Fig. 1. Taking the difference between the two detector outputs rejects essentially all the 1/f noise from the amplifiers. A 180° phase switch, between the magic tees, flips the assignment of the detectors to the radiometer inputs, and phase switch demodulation rejects the 1/f noise in the detectors and post-detector electronics, at frequencies less than the phase switching frequency.

This memo reviews the design considerations for the continuum section of the radiometer. This is actually a very coarse resolution spectrometer, with 3 channels covering the 26-40 GHz band. The intent is to provide the background for a more detailed design and cost analysis. The emphasis in this design is on flux density and spectral index measurements of weak point sources, in the range a few x 100 μJy to a few x 10 mJy, to support CBI observations.

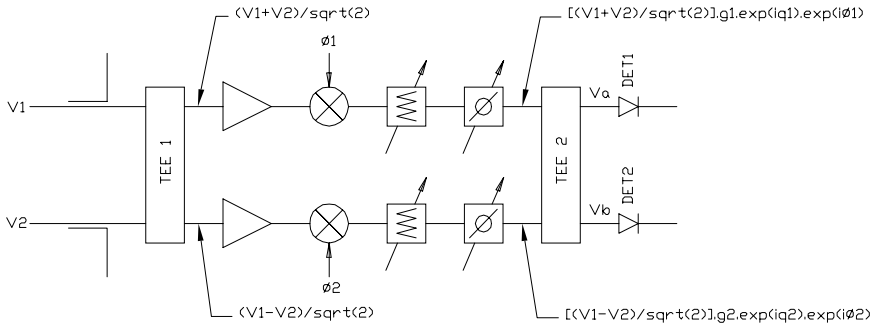

Figure 1: Differential radiometer.

II. Design tolerances

This section contains an analysis of the radiometer performance. The main results are summarized in Figures 2 and 3 and in the last paragraph of this section.

Differential passband errors, in the components between the two magic tees, degrade the sensitivity and cause leakage between the radiometer arms. In Fig. 1, the voltage gain of the com-

ponents between the magic tees in the upper arm is $G_u = g_1.e^{iq_1}.e^{i\phi_1}$, where q_1 is the passband phase error and ϕ_1 is the phase introduced by the phase switch. The voltage gain of the lower arm is $G_l = g_2.e^{iq_2}.e^{i\phi_2}$.

Detector 1 input $V_a = \frac{G_u}{\sqrt{2}}(\frac{V_1}{\sqrt{2}} + \frac{V_2}{\sqrt{2}}) + \frac{G_l}{\sqrt{2}}(\frac{V_1}{\sqrt{2}} - \frac{V_2}{\sqrt{2}})$

Detector 2 input $V_b = \frac{G_u}{\sqrt{2}}(\frac{V_1}{\sqrt{2}} + \frac{V_2}{\sqrt{2}}) - \frac{G_l}{\sqrt{2}}(\frac{V_1}{\sqrt{2}} - \frac{V_2}{\sqrt{2}})$

If d_1 is the gain (volts/watt) of detector 1, detector 1 output is:

$d_1 V_a V_a^* = \frac{d_1}{2}[G_u(\frac{V_1}{\sqrt{2}} + \frac{V_2}{\sqrt{2}}) + G_l(\frac{V_1}{\sqrt{2}} - \frac{V_2}{\sqrt{2}})].[G_u^*(\frac{V_1^*}{\sqrt{2}} + \frac{V_2^*}{\sqrt{2}}) + G_l^*(\frac{V_1^*}{\sqrt{2}} - \frac{V_2^*}{\sqrt{2}})]$

$= \frac{d_1}{2}[|G_u|^2(\frac{V_1}{\sqrt{2}}+\frac{V_2}{\sqrt{2}})(\frac{V_1^*}{\sqrt{2}}+\frac{V_2^*}{\sqrt{2}})+|G_l|^2(\frac{V_1}{\sqrt{2}}-\frac{V_2}{\sqrt{2}})(\frac{V_1^*}{\sqrt{2}}-\frac{V_2^*}{\sqrt{2}})+G_uG_l^*(\frac{V_1}{\sqrt{2}}+\frac{V_2}{\sqrt{2}})(\frac{V_1^*}{\sqrt{2}}-\frac{V_2^*}{\sqrt{2}})+G_u^*G_l(\frac{V_1}{\sqrt{2}}-\frac{V_2}{\sqrt{2}})(\frac{V_1^*}{\sqrt{2}}+\frac{V_2^*}{\sqrt{2}})]$

$= \frac{d_1}{4}[(|V_1|^2+|V_2|^2)(|G_u|^2+|G_l|^2)+(V_1V_2^*+V_1^*V_2)(|G_u|^2-|G_l|^2)+(|V_1|^2-|V_2|^2)(G_uG_l^*+G_u^*G_l)+(V_1^*V_2-V_1V_2^*)(G_uG_l^*-G_u^*G_l)]$

In the ideal case, $|G_u| = |G_l| = g$, and $q_1 = q_2 = 0$.

If $\phi_1 - \phi_2 = \Delta\phi$, then $G_uG_l^* + G_u^*G_l = 2g^2\cos\Delta\phi$

and $d_1V_aV_a^* = \frac{g^2d_1}{2}[(|V_1|^2+|V_2|^2)+(|V_1|^2-|V_2|^2)\cos\Delta\phi]$

If $\Delta\phi = 0$, $d_1V_aV_a^* = g^2d_1|V_1|^2$, if $\Delta\phi = \pi$, $d_1V_aV_a^* = g^2d_1|V_2|^2$,

and if $\Delta\phi = \frac{\pi}{2}$, $d_1V_aV_a^* = \frac{g^2d_1(|V_1|^2+|V_2|^2)}{2}$

Detector 2 output is:

$d_2 V_b V_b^* = \frac{d_2}{2}[G_u(\frac{V_1}{\sqrt{2}} + \frac{V_2}{\sqrt{2}}) - G_l(\frac{V_1}{\sqrt{2}} - \frac{V_2}{\sqrt{2}})].[G_u^*(\frac{V_1^*}{\sqrt{2}} + \frac{V_2^*}{\sqrt{2}}) - G_l^*(\frac{V_1^*}{\sqrt{2}} - \frac{V_2^*}{\sqrt{2}})]$

$= \frac{d_2}{2}[|G_u|^2(\frac{V_1}{\sqrt{2}}+\frac{V_2}{\sqrt{2}})(\frac{V_1^*}{\sqrt{2}}+\frac{V_2^*}{\sqrt{2}})+|G_l|^2(\frac{V_1}{\sqrt{2}}-\frac{V_2}{\sqrt{2}})(\frac{V_1^*}{\sqrt{2}}-\frac{V_2^*}{\sqrt{2}})-G_uG_l^*(\frac{V_1}{\sqrt{2}}+\frac{V_2}{\sqrt{2}})(\frac{V_1^*}{\sqrt{2}}-\frac{V_2^*}{\sqrt{2}})-G_u^*G_l(\frac{V_1}{\sqrt{2}}-\frac{V_2}{\sqrt{2}})(\frac{V_1^*}{\sqrt{2}}+\frac{V_2^*}{\sqrt{2}})]$

$= \frac{d_2}{4}[(|V_1|^2+|V_2|^2)(|G_u|^2+|G_l|^2)+(V_1V_2^*+V_1^*V_2)(|G_u|^2-|G_l|^2)-(|V_1|^2-|V_2|^2)(G_uG_l^*+G_u^*G_l)-(V_1^*V_2-V_1V_2^*)(G_uG_l^*-G_u^*G_l)]$

In the ideal case, $|G_u| = |G_l| = g$, and $q_1 = q_2 = 0$.

If $\phi_1 - \phi_2 = \Delta\phi$, then $G_uG_l^* + G_u^*G_l = 2g^2\cos\Delta\phi$

and $V_bV_b^* = \frac{g^2d_2}{2}[(|V_1|^2+|V_2|^2)-(|V_1|^2-|V_2|^2)\cos\Delta\phi]$

If $\Delta\phi = 0$, $d_2V_bV_b^* = g^2d_2|V_2|^2$, if $\Delta\phi = \pi$, $d_2V_bV_b^* = g^2d_2|V_1|^2$,

and if $\Delta\phi = \frac{\pi}{2}$, $d_2V_bV_b^* = \frac{g^2d_2(|V_1|^2+|V_2|^2)}{2}$

A. Total power mode

For total power observations, we will take the time average of one of the detector outputs, with the phase switch off (i.e. G_u and G_l constant). In this mode, the radiometer is equivalent to a simple total power system, with one amplifier and one detector, and there is no rejection of 1/f noise. For astronomical observations, V_1 and V_2 are uncorrelated, so $< V_1^* V_2 >= 0$ etc. Detector 1 output is then:

$< d_1 V_a V_a^* >=< \frac{d_1}{4}[(|V_1|^2 + |V_2|^2)(|G_u|^2 + |G_l|^2) + (|V_1|^2 - |V_2|^2)(G_u G_l^* + G_u^* G_l)] >$

$= d_1 < \frac{|V_1|^2}{4}[|G_u|^2 + |G_l|^2 + G_u G_l^* + G_u^* G_l] + \frac{|V_2|^2}{4}[|G_u|^2 + |G_l|^2 - G_u G_l^* - G_u^* G_l] >$

$= d_1 < \frac{|V_1|^2}{4}(G_u + G_l)(G_u^* + G_l^*) + \frac{|V_2|^2}{4}(G_u - G_l)(G_u^* - G_l^*) >$

$= d_1 < \frac{|V_1|^2}{4}|G_u + G_l|^2 + \frac{|V_2|^2}{4}|G_u - G_l|^2 >$

The response of the radiometer in total power mode has the expected term in $|V_1|^2$, and also a term in $|V_2|^2$ due to leakage between the two arms. The normalized leakage from input 2 to detector 1 is:

$L_{12} = \frac{|G_u - G_l|^2}{|G_u + G_l|^2}$ and if $\frac{G_l}{G_u} = G$, $L_{12} = \frac{|1-G|^2}{|1+G|^2}$, which is shown in Fig. 2.

The rms noise voltage at the output of detector 1 due to noise from the amplifiers is:

$N_1 = d_1 \frac{kB}{\sqrt{B\tau}}(T_{amp\_u}\frac{|G_u|^2}{2} + T_{amp\_l}\frac{|G_l|^2}{2})$, where B is the detector input bandwidth, τ is the integration time and T_{amp_u} and T_{amp_l} are the noise temperatures of the amplifiers in the upper and lower arms, respectively.

If $T_{amp\_u} = T_{amp\_l} = T_{amp}$, then $N_1 = d_1 \frac{kB}{\sqrt{B\tau}}\frac{T_{amp}}{2}[|G_u|^2 + |G_l|^2]$.

From our expression for the time average of detector 1 output, the dc voltage at detector 1 due to T_1 at input 1 is $d_1 kBT_1\frac{|G_u+G_l|^2}{4}$

To measure the radiometer noise temperature, T_r, we put a load at T_r at input 1, and integrate for time $\tau = \frac{1}{B}$. Then,

$d_1 kBT_r\frac{|G_u+G_l|^2}{4} = d_1 kB\frac{Tamp}{2}[|G_u|^2 + |G_l|^2]$

and $T_r = 2T_{amp}\frac{|G_u|^2+|G_l|^2}{|G_u+G_l|^2} = 2T_{amp}\frac{1+|G|^2}{|1+G|^2}$.

The sensitivity degradation, relative to a simple total power radiometer, is $\frac{T_r}{T_{amp}} = 2\frac{1+|G|^2}{|1+G|^2}$. This is shown in Fig. 2.

In the ideal case $G_u = G_l$, so $G = 1$ and $T_r = T_{amp}$, as expected. If the lower amplifier dies, so $G_u = 1$ and $G_l = 0$, $G = 0$, $L_{12} = 1$ and $T_r = 2T_{amp}$.

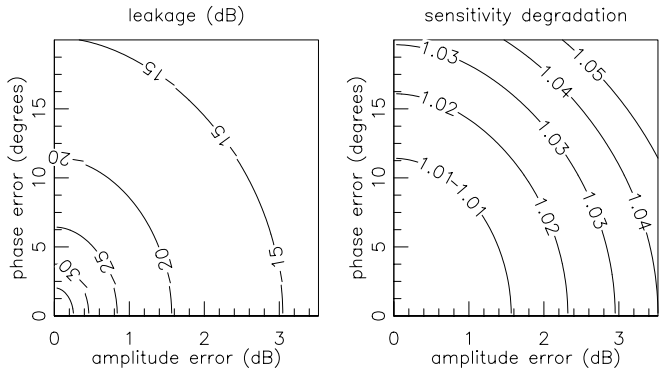

Figure 2: Leakage and sensitivity degradation due to differential passband errors between the two arms of the radiometer, in total power mode.

B. Differential mode

In differential mode, we will take the time average of the difference between the detector outputs:

$< d_1 V_a V_a^* - d_2 V_b V_b^* >$

$=< \frac{1}{4}[(d_1 - d_2)(|V_1|^2 + |V_2|^2)(|G_u|^2 + |G_l|^2) + (d_1 - d_2)(V_1 V_2^* + V_1^* V_2)(|G_u|^2 - |G_l|^2) + (d_1 + d_2)(|V_1|^2 - |V_2|^2)(G_u G_l^* + G_u^* G_l) + (d_1 + d_2)(V_1^* V_2 - V_1 V_2^*)(G_u G_l^* - G_u^* G_l)] >$

Now,

$G_u G_l^* + G_u^* G_l = g_1.e^{i(q_1+\phi_1)} g_2.e^{-i(q_2+\phi_2)} + g_1.e^{-i(q_1+\phi_1)} g_2.e^{i(q_2+\phi_2)}$

$= g_1.g_2.[e^{i(\Delta q+\Delta\phi)} + e^{-i(\Delta q+\Delta\phi)}]$

$= 2.g_1.g_2 \cos(\Delta q + \Delta\phi)$, where $\Delta q = q_1 - q_2$ and $\Delta\phi = \phi_1 - \phi_2$.

V_1 and V_2 are uncorrelated, so $< V_1^* V_2 >= 0$ etc. Then,

$< d_1 V_a V_a^* - d_2 V_b V_b^* >$

$=< \frac{1}{4}[(d_1 - d_2)(|V_1|^2 + |V_2|^2)(|G_u|^2 + |G_l|^2) + 2(d_1 + d_2)(|V_1|^2 - |V_2|^2).g_1.g_2 \cos(\Delta q + \Delta\phi)] >$

This has the expected $(|V_1|^2 - |V_2|^2)$ term, and also a term in $(|V_1|^2 + |V_2|^2)$ due to the difference in the detector gains.

In differential mode, we will operate the phase switch to reject 1/f noise in the detectors and

to remove the $(|V_1|^2 + |V_2|^2)$ response of the radiometer. The radiometer outputs for the 0° and 180° phase switch states are:

$< d_1 V_a V_a^* - d_2 V_b V_b^* >_{\Delta\phi=0} = < \frac{1}{4}[(d_1 - d_2)(|V_1|^2 + |V_2|^2)(|G_u|^2 + |G_l|^2) + 2(d_1 + d_2)(|V_1|^2 - |V_2|^2).g_1.g_2 \cos(\Delta q)] >$

$< d_1 V_a V_a^* - d_2 V_b V_b^* >_{\Delta\phi=\pi} = < \frac{1}{4}[(d_1 - d_2)(|V_1|^2 + |V_2|^2)(|G_u|^2 + |G_l|^2) - 2(d_1 + d_2)(|V_1|^2 - |V_2|^2).g_1.g_2 \cos(\Delta q)] >$

Taking the difference between the two phase switch states, and dividing by 2 to normalize, gives:

$\frac{1}{2}[< d_1 V_a V_a^* - d_2 V_b V_b^* >_{\Delta\phi=0} - < d_1 V_a V_a^* - d_2 V_b V_b^* >_{\Delta\phi=\pi}] = < \frac{1}{2}(d_1 + d_2)(|V_1|^2 - |V_2|^2).g_1.g_2 \cos(\Delta q) >$

which contains terms only in $|V_1|^2 - |V_2|^2$.

In the ideal case, $d_1 = d_2 = d$, $g_1 = g_2 = g$ and $\Delta q = 0$. Then,

$\frac{1}{2}[< dV_a V_a^* - dV_b V_b^* >_{\Delta\phi=0} - < dV_a V_a^* - dV_b V_b^* >_{\Delta\phi=\pi}] = < d(|V_1|^2 - |V_2|^2)g^2 >$

With ideal phase switches, the rms noise voltage at the detector outputs is the same as in the total power case:

$N_1 = d_1 \frac{kB}{\sqrt{B\tau}} \frac{T_{amp}}{2}[|G_u|^2 + |G_l|^2]$ for detector 1,

and $N_2 = d_2 \frac{kB}{\sqrt{B\tau}} \frac{T_{amp}}{2}[|G_u|^2 + |G_l|^2]$ for detector 2.

The rms noise voltage on the difference between the two detector outputs is:

$N_{1-2} = \frac{kB}{\sqrt{B\tau}} \frac{T_{amp}}{2} \sqrt{d_1^2 + d_2^2}[|G_u|^2 + |G_l|^2]$

The noise is the same for both phase switch states, so the rms noise voltage after differencing between the two states (remembering we divide by 2 to normalize) is:

$N = \frac{kB}{\sqrt{B\tau}} \frac{T_{amp}}{2} \sqrt{\frac{d_1^2 + d_2^2}{2}}[|G_u|^2 + |G_l|^2]$

The radiometer dc output (after phase switch demodulation) due to T_1 at input 1 is

$\frac{1}{2}(d_1 + d_2)kBT_1.g_1.g_2 \cos(\Delta q)$

As before, we calculate the radiometer noise temperature by setting $T_1 = T_r$ and $B\tau = 1$. Then,

$\frac{1}{2}(d_1 + d_2)kBT_r.g_1.g_2 \cos(\Delta q) = kB \frac{T_{amp}}{2} \sqrt{\frac{d_1^2 + d_2^2}{2}}[|G_u|^2 + |G_l|^2]$

and $T_r = T_{amp} \frac{\sqrt{d_1^2 + d_2^2}[|G_u|^2 + |G_l|^2]}{\sqrt{2}(d_1 + d_2).g_1.g_2 \cos(\Delta q)} = T_{amp} \frac{\sqrt{d_1^2 + d_2^2}[g_1^2 + g_2^2]}{\sqrt{2}(d_1 + d_2).g_1.g_2 \cos(\Delta q)}$

In the ideal case, $d_1 = d_2 = d$, $g_1 = g_2 = g$ and $\Delta q = 0$, giving $T_r = T_{amp}$.

The sensitivity degradation due to differential passband errors is $D_g = \frac{g_1^2 + g_2^2}{2.g_1.g_2 \cos(\Delta q)} = \frac{1 + (\frac{g_2}{g_1})^2}{2(\frac{g_2}{g_1}) \cos(\Delta q)}$

which is shown in Fig. 3. The sensitivity degradation due to gain differences between the detectors is $D_d = \frac{\sqrt{2(d_1^2+d_2^2)}}{(d_1+d_2)} = \frac{\sqrt{2(1+(\frac{d_2}{d_1})^2)}}{(1+\frac{d_2}{d_1})}$. Since phase switching shares the signals between both detectors, and the detector gains affect both the signal and the noise, even large detector gain differences do not seriously degrade the radiometer sensitivity. e.g. if $\frac{d_2}{d_1} = 2$, $D_d = 1.05$. If the lower detector dies, $d_2 = 0$ and $D_d = \sqrt{2}$. This is expected, because with only the upper detector working, phase switching causes the system to operate as a Dicke radiometer. The working detector spends half the time sampling each radiometer input, so the sensitivity of the system is reduced by $\sqrt{2}$. Since the performance of the radiometer is not very sensitive to detector gain differences, we do not have to accurately set the detector input powers, or accurately adjust the gains of the post-detector amplifiers. This gives us the option of computing the difference between the detector outputs in hardware (using an operational amplifier), rather than in software.

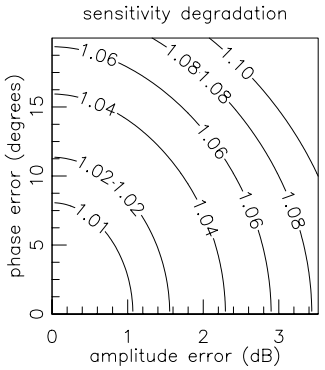

Figure 3: Sensitivity degradation due to differential passband errors between the two arms of the radiometer, in phase switched differential mode.

So far, we have considered a radiometer with ideal phase switches, but for a real phase switch, the passband errors depend on the state of the switch. We might expect the sensitivity degradation due to phase switch errors to be about half that due to similar differential passband errors between the two arms of the radiometer. Half, because the phase switch spends half its time in each state. If $p_1(\Delta\phi)$ is the gain of the upper arm phase switch, and $p_2(\Delta\phi)$ is the gain of the lower arm phase switch, $G_u = p_1(\Delta\phi).g_1.e^{iq_1}.e^{i\phi_1}$ and $G_l = p_2(\Delta\phi).g_2.e^{iq_2}.e^{i\phi_2}$. For simplicity, assume that p_1 and p_2 are real i.e. there are no phase errors in the phase switches. Then, the difference between the

detector outputs is:

$< d_1 V_a V_a^* - d_2 V_b V_b^* >$

$=< \frac{1}{4}[(d_1 - d_2)(|V_1|^2 + |V_2|^2)(|G_u|^2 + |G_l|^2) + 2(d_1 + d_2)(|V_1|^2 - |V_2|^2).g_1.g_2.p_1(\Delta\phi).p_2(\Delta\phi)\cos(\Delta q + \Delta\phi)] >$

The radiometer output for the two phase switch states is:

$< (d_1 V_a V_a^* - d_2 V_b V_b^*)_{\Delta\phi=0} >$

$=< \frac{1}{4}[(d_1 - d_2)(|V_1|^2 + |V_2|^2)(|G_u|^2 + |G_l|^2) + 2(d_1 + d_2)(|V_1|^2 - |V_2|^2).g_1.g_2.p_1(0).p_2(0)\cos(\Delta q)] >$

and $< (d_1 V_a V_a^* - d_2 V_b V_b^*)_{\Delta\phi=\pi} >$

$=< \frac{1}{4}[(d_1 - d_2)(|V_1|^2 + |V_2|^2)(|G_u|^2 + |G_l|^2) - 2(d_1 + d_2)(|V_1|^2 - |V_2|^2).g_1.g_2.p_1(\pi).p_2(\pi)\cos(\Delta q)] >$

Taking the difference between the two states, and dividing by 2, gives:

$\frac{1}{2}[< d_1 V_a V_a^* - d_2 V_b V_b^* >_{\Delta\phi=0} - < d_1 V_a V_a^* - d_2 V_b V_b^* >_{\Delta\phi=\pi}]$

$=< \frac{1}{2}(d_1 + d_2)(|V_1|^2 - |V_2|^2).g_1.g_2.[p_1(0).p_2(0) + p_1(\pi).p_2(\pi)]\cos(\Delta q) >$

so the phase dependent gain in the phase switches just causes a scale factor error of

$[p_1(0).p_2(0) + p_1(\pi).p_2(\pi)]$.

The rms noise voltage on the difference between the two detector outputs is:

$N_{1-2(\Delta\phi=0)} = \frac{kB}{\sqrt{B\tau}} \frac{T_{amp}}{2} \sqrt{d_1^2 + d_2^2}[|G_u|^2 p_1^2(0) + |G_l|^2 p_2^2(0)]$

$N_{1-2(\Delta\phi=\pi)} = \frac{kB}{\sqrt{B\tau}} \frac{T_{amp}}{2} \sqrt{d_1^2 + d_2^2}[|G_u|^2 p_1^2(\pi) + |G_l|^2 p_2^2(\pi)]$

and after phase switch demodulation, the radiometer output noise is:

$N = \frac{kB}{\sqrt{B\tau}} \frac{T_{amp}}{2} \sqrt{\frac{d_1^2 + d_2^2}{4}\{[|G_u|^2 p_1^2(0) + |G_l|^2 p_2^2(0)]^2 + [|G_u|^2 p_1^2(\pi) + |G_l|^2 p_2^2(\pi)]^2\}}$

If $|G_u| = |G_l|$, the sensitivity degradation due to the phase switch errors is:

$D_p = \frac{\sqrt{[p_1^2(0) + p_2^2(0)]^2 + [p_1^2(\pi) + p_2^2(\pi)]^2}}{\sqrt{2}[p_1(0).p_2(0) + p_1(\pi).p_2(\pi)]}$

Since errors in the phase switch gains affect both the signal and the noise, the sensitivity degradation is small, even for quite large errors. If $p_1(0) = p_2(0) = 1$ and $p_1(\pi) = p_2(\pi) = 1.413$ (i.e. 3 dB gain error), $D_p = 1.05$.

Fig. 2 indicates that in total power mode, for $< 1\%$ leakage and $< 1\%$ sensitivity degradation, we must keep differential passband errors below ~ 1.5 dB and $10°$. In phase switched differential mode, the tolerances are a little tighter, and passband errors should be below $\sim$1 dB and $7°$

for $< 1\%$ sensitivity degradation. This will probably be very difficult over the full 26–40 GHz band, and we will likely be forced to accept larger passband errors. Fortunately, the leakage and sensitivity degradation do not increase very rapidly with passband error. 3 dB or 20° errors still give good performance, with 3% leakage and 3% sensitivity degradation in total power mode, and 6% sensitivity degradation in phase switched differential mode.

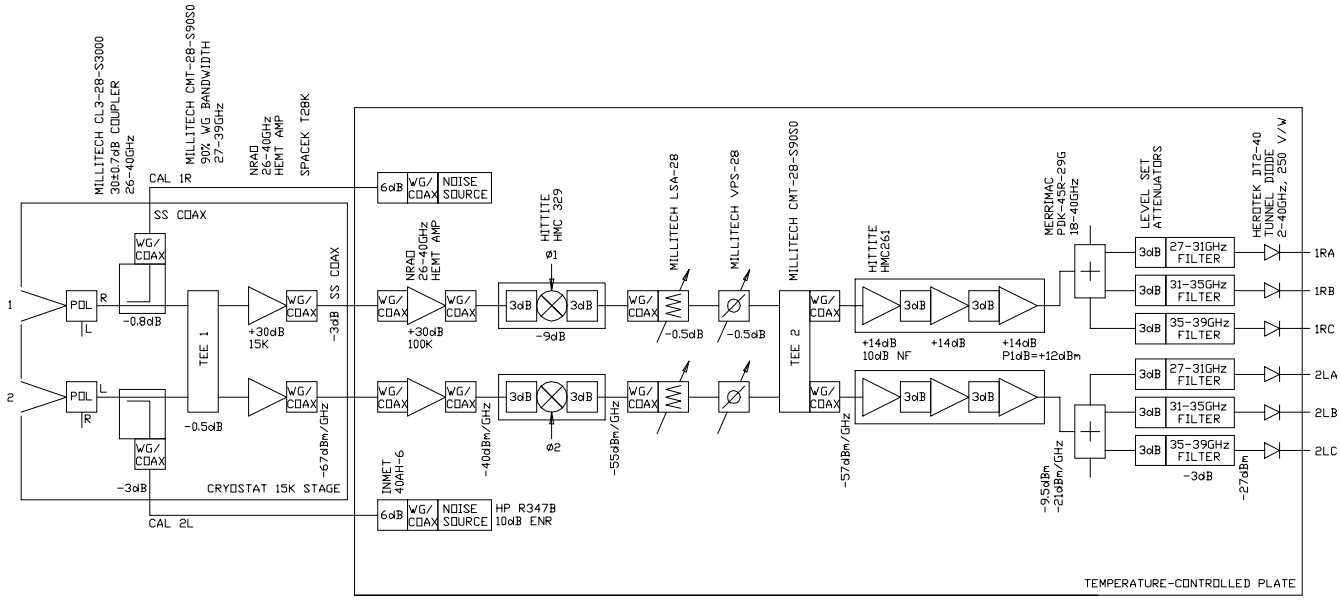

Figure 4: Radiometer front end. This diagram shows the details for just one polarization (horn1Right–horn2Left). The circuit for the other polarization is identical.

III. Front end

Fig. 4 shows a possible arrangement for the radiometer front end. This design attempts to minimize the number of components between the magic tees, to reduce the differential passband errors. The diagram shows specific components, but these may not be the best choices. The intent is only to show that appropriate parts are available.

For point source observations, we would like a small separation between the two radiometer beams to maximize the rejection of atmospheric noise. A separation of ~ 2 beamwidths would give a good compromise between beam overlap and atmospheric noise rejection. The GBT secondary

subtends a half angle of 15° at the secondary focus [2], and for ~ -12 dB edge taper we need a corrugated horn with a semi-flare angle of $\sim 20°$ [3]. For constant beamwidth over the 26-40 GHz band, the diameter of the horn should be $\sim 7\lambda$ at 26 GHz. The minimum possible spacing between horns is then ~ 9 cm, which gives a beam separation of ~ 1.6' (for a focal length of 190 m). The beamwidth of the GBT at 40 GHz is ~ 0.60' (assuming 30% aperture efficiency), so the beam separation is ~ 2.7 beamwidths. At 26 GHz, the beam separation is ~ 1.7 beamwidths.

Fig. 4 shows a polarizer at each feedhorn. This assembly will likely be a circular polarizer and an orthomode junction. Circular polarization seems to be the best choice, since it minimizes the effect of linearly polarized foregrounds, and is used for VLBI observations. Cross-talk between the feeds is minimized if we difference orthogonal polarizations as in Fig. 4. The feedhorns and polarizers will be supplied by NRAO CDL. The front end optics may also include a cold absorber-style calibrator, but this is uncertain. Each input of the radiometer has a directional coupler for injecting a noise calibration signal. The coupling is -30 dB, so terminating the calibration port with a room temperature load increases the receiver noise by only 0.3 K. In Fig. 4, the calibration signal is only ~ 0.3 K, and we may want to include a brighter calibration source for testing isolation and linearity.

The magic tees in Fig. 4 limit the bandwidth of the radiometer to 90% of the full waveguide band. This seems to be typical of the commercially available tees, but we may be able to find a design for a wider band tee, if it is important to cover the full 26–40 GHz. Between the tees, each arm of the radiometer has two NRAO InP HEMT amplifiers, a phase switch and a variable attenuator and phase shifter. We could correct passband differences by adding fixed attenuators and delay lines, but for a single receiver, it is easy and convenient to include the adjustable attenuators and phase shifters. The 180° phase switches are double-balanced mixers. These have wideband IF ports, so very fast phase switching is possible, and if the diodes and baluns in the mixers are well matched, the passband errors for the two switch states are similar. Fig. 4 shows Hittite MMIC mixers, with 3 dB attenuators to reduce reflections, but Miteq also makes a packaged mixer (DB0440LW1) that would work well. With ± 10 mA IF port bias current, the

Miteq mixer has $\sim$ 0.8 dB and 10°–15° deviations from a 180° phase shift, over the 26–40 GHz band. Unfortunately, double-balanced mixers are quite lossy, so two NRAO HEMT amplifiers must precede the phase switch. With just one amplifier before the phase switch, the noise contribution from the second amplifier is $\sim$ 6 K (assuming a noise temperature of 100 K for the second amplifier, and 18 dB loss for the mixer, 3 dB attenuators and the coaxial cables in the cryostat). This is much worse than the noise temperature degradation due to the differential passband errors introduced by putting the second amplifier between the magic tees. Putting both InP HEMT amplifiers between the magic tees will also reduce the 1/f noise for the radiometer, if the InP HEMT amplifiers have significant 1/f noise at the phase switching frequency. Two NRAO InP HEMT amplifiers do not provide enough gain for the radiometer, so Fig. 4 shows GaAs MMIC amplifiers at the outputs of the second magic tee. Since these amplifiers are outside the magic tees, their 1/f noise is rejected only by phase switching. GaAs amplifiers have lower 1/f noise than InP amplifiers, so outside the magic tees, it is better to use GaAs amplifiers. If 1/f noise from the GaAs amplifiers is a problem, we may be able to select amplifiers with similar passband errors and put them between the magic tees.

Following the GaAs MMIC amplifiers there is a simple 3-channel filterbank, with attenuators for each filter to set the appropriate power level for the detectors. If the detectors require an external dc return, we may have to include a 1 dB attenuator at the output of each filter. Phase switching time-shares the signals between the filters in the two arms of the radiometer, so the effective passband for a channel is the average of the passbands of the two filters. Differences between the filter passbands reduce the effective bandwidth of the channel, but since the sensitivity is proportional to $\sqrt{B}$, the filter passbands do not need to be very well matched. The power splitters that feed the filters have a spare output for a connection to a downcoverter for the GBT spectrometer. All the components outside the cryostat are mounted on a temperature-controlled plate, and based on our experience with the OVRO radiometers, temperature control to $\sim \pm 100$ mK is adequate.

Fig. 4 shows coax connections for all the signals entering and leaving the cryostat. Coax is

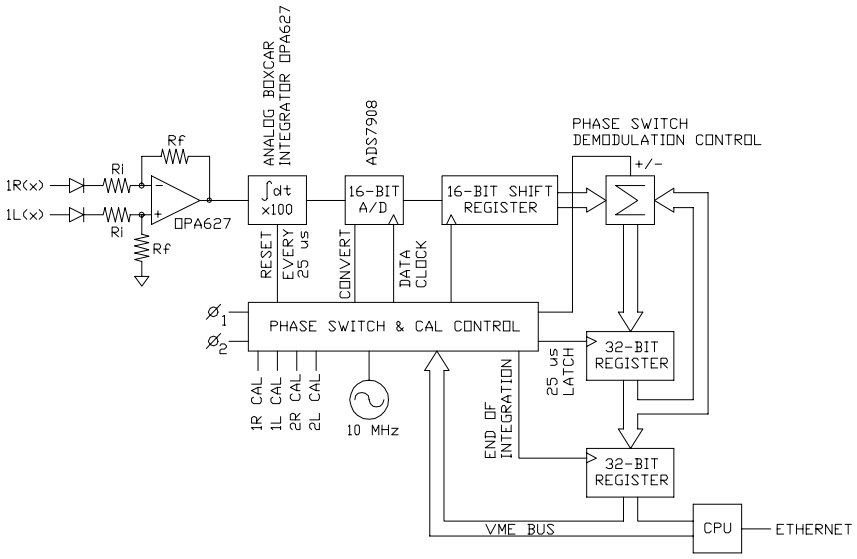

Figure 5: Detector readout for one frequency channel.

fairly easy to reconfigure and the loss in the stainless steel lines inside the cryostat helps to reduce reflections. Radiall makes 2.9-mm hermetic bulkhead adapters, which we use for 26-38 GHz signals in the CBI cryostats. The size of the cryostat will be determined largely by whether or not we decide to cool the feedhorns. The horn throats certainly should be cooled, but the flare sections could be at room temperature. DASI uses this approach for its 26-36 GHz horns, and we could probably adopt the same thermal break design. If only the horn throats are cooled, a CTI 350 refrigerator will probably be adequate.

IV. Detector readout

Fig. 5 shows a detector readout circuit for one channel in the radiometer. This particular design is based on the readout electronics for the analog correlator in the CBI, but there are other options. For example, we could use a single A/D converter preceded by an analog multiplexer, instead of having an A/D for each channel. We could also do the phase switch demodulation in software, instead of having a hardware digital signal processor. The details for all these schemes are quite different, but the overall design considerations are similar.

In Fig. 5, the detector outputs are differenced immediately, in hardware. An advantage of

this approach is that it removes the dc components due to the receiver noise, and this reduces the dynamic range required in the post-detector amplifiers and the A/D. The effects of temperature dependent offsets in the detectors are also minimized, and the component count is low. However, the scheme precludes total power operation, and a problem with the output of one of the detectors might be difficult to find. We could use a separate readout circuit for each detector and take the difference in software. For total power operation, it would probably be best to make a differential measurement between two detectors, one connected to the radiometer output and the other connected to a load. If the two detectors are in good thermal contact, taking the difference between their outputs rejects temperature dependent offset variations. The disadvantage of this approach is that it doubles the number of detectors in the system.

In the circuit of Fig. 5, the noise at a detector output (in V^2/Hz) is:

$V_n^2 = \frac{V_{dc}^2}{B} + e_n^2 + R_i^2 i_n^2 + (\frac{4kT_o}{R_i})R_i^2 + (\frac{4kT_o}{R_f})R_i^2 + (\frac{V_{fs}}{2^n}\frac{R_i}{R_f}\frac{1}{a_{int}})^2\tau$

where V_{dc} is the detector dc output voltage due to the radiometer noise, e_n ($\mathrm{V}/\sqrt{\mathrm{Hz}}$) and i_n ($\mathrm{A}/\sqrt{\mathrm{Hz}}$) are the opamp input noise voltage and current, V_{fs} is the full-scale input for the A/D, n is the number of bits in the A/D, a_{int} is the gain of the boxcar integrator and τ is the integration time (τ is equal to the phase switch period). The first term in this expression is just the detector output noise due to the radiometer noise; the 2nd and 3rd terms are the opamp input noise [4]; the 4th and 5th terms are Johnson noise from the resistors in the post-detector amplifier; and the last term is the quantization noise from the A/D, divided by the gain of the post-detector amplifier and integrator. If we set $V_{fs} = 2a_{int}\frac{R_f}{R_i}V_{dc}$ (i.e. full-scale for the A/D corresponds to twice the detector dc output voltage), then

$V_n^2 = \frac{V_{dc}^2}{B} + e_n^2 + R_i^2 i_n^2 + 4kT_oR_i + (\frac{4kT_o}{R_f})R_i^2 + \frac{V_{dc}^2\tau}{2^{2(n-1)}}$

Noise from the readout electronics is rejected for frequencies less than the phase switching frequency, so it is advantageous to switch as fast as possible. The A/D conversion time limits the phase switch period to $\gtrsim 10$ μs. In the readout for the CBI correlator, we use a minimum phase switch period of 25.6 μs ($2^8 \div 10$ MHz), and this value has been adopted for the following discussion. If we sample all combinations of the settings of the two phase switches in the radiometer, a complete

phase switching cycle has 4 states, and the minimum possible readout time for the radiometer is $\sim$ 100 μs. With this cycle time, readout noise at frequencies $\lesssim$ 10 kHz is rejected by phase switching.

From Fig. 4, the detector input power is ~ -27 dBm, and assuming $d = 0.25$ V/mW, the dc output voltage is ~ 0.5 mV. The typical full-scale input for an A/D is ~ 5 V, so for total power operation we need a post-detector gain of $\sim 10^4$. This is too much for a single opamp stage at the detector output, because the minimum load resistance (R_i) for the detector is ~ 10 kΩ. However, we can split the gain between the post-detector amplifier and integrator stages. If the amplifier gain is 100 and $R_i = 10$ kΩ, then $R_f = 1$ MΩ. An analog boxcar integrator with a gain of 100 and $\tau = 25$ μs requires an RC product of 2.5x10^{-7} (e.g. $R = 1$ kΩ and $C = 250$ pF). The radiometer output must be blanked during phase switch transitions, and this can done using the integrator reset control. With a 25 μs phase switch period, we would probably blank for ~ 0.5 μs, which reduces the integration time by 2% and degrades the sensitivity of the radiometer by 1%. In 0.5 μs, the post-detector amplifier output must change by ~ 100 mV, so we need an opamp with a slew rate of at least 0.2 V μs^{-1}. The integrator output must slew ~ 10 V in 0.5 μs, i.e. 20 V μs^{-1}. The design in Fig. 5 uses Burr-Brown OPA627 opamps, which have 40 V μs^{-1} slew rate and very low noise. At 10 kHz, $e_n = 6$ nV/$\sqrt{\text{Hz}}$ and at 100 Hz, $i_n = 2.5$ fA/$\sqrt{\text{Hz}}$ (i_n will be lower at 10 kHz, but the value is not given on the opamp data sheet).

The quantization noise in the A/D must be small compared with the radiometer output noise, i.e. $\frac{V_{dc}^2 \tau}{2^{2(n-1)}} < \frac{V_{dc}^2}{B}$, so $2^{2(n-1)} > B\tau$ and $n > 1 + \log_2 \sqrt{B\tau}$. With $B = 4$ GHz and $\tau = 25$ μs, $n > 10$. In the CBI correlator, we use Burr-Brown ADS7809 16-bit A/Ds. These have $\sim$10 μs conversion time, and taking into account non-linearities, the effective number of bits is $\sim$13.

We have now specified enough details in the readout circuit to calculate the various noise contributions at the detector output:

	$V^2/\sqrt{\text{Hz}}$		$\text{nV}/\sqrt{\text{Hz}}$
radiometer noise	$\frac{V_{dc}^2}{B}$	$V_{dc} = 5$ mV, $B = 4$ GHz	79
opamp noise voltage (at 10 kHz)	e_n^2	$e_n = 6\ \text{nV}/\sqrt{\text{Hz}}$	6
opamp noise current (at 100 Hz)	$R_i^2 i_n^2$	$R_i = 10\ \text{k}\Omega$, $i_n = 2.5\ \text{fA}/\sqrt{\text{Hz}}$	0.03
Johnson noise in R_i	$4kT_oR_i$	$R_i = 10\ \text{k}\Omega$, $T_o = 290$ K	12.6
Johnson noise in R_f	$(\frac{4kT_o}{R_f})R_i^2$	$R_i = 10\ \text{k}\Omega$, $R_f = 1\ \text{M}\Omega$, $T_o = 290$ K	1.3
A/D quantization noise	$\frac{V_{dc}^2\tau}{2^{2(n-1)}}$	$V_{dc} = 5$ mV, $\tau = 25\ \mu$s, $n = 13$	6.1
		total noise	80.5

The sensitivity degradation due to the post-detector electronics is $\sim 2\%$, mainly from the Johnson noise in the detector load resistor. We could probably reduce this by a factor of 2 without significantly decreasing the detector gain.

The signal processing after the A/D consists of a digital integrator and phase switch demodulator. Fig. 5 shows a hardware implementation, but we could also handle this in software. The hardware approach is quite straightforward, and the electronics for all six channels in the radiometer, including the control circuits for the A/Ds, integrators and phase switches, would fit into a single Altera EPF10K50 field-programmable gate array. In Fig. 5, the CPU handles all the radiometer interfaces, and the only connection to the outside world is via ethernet. This approach would allow us to load a data acquisition package, such as LabView, into the CPU for testing the radiometer. For real observations, the CPU might be just a data buffer, or it could handle higher-level operations, for example returning flux densities from a beam switched observation. An attractive possibility for the electronics is to design a circuit board with the readout, control and monitoring for the complete radiometer on a single board. This would be quite a complicated board, but it would eliminate a lot of interface wiring, and could be used for other differential radiometers for the GBT.

V. Discussion

Before proceeding with a detailed design of the front end and cryostat, the feedhorns must be designed, and in particular, we must decide whether or not to cool the flare sections of the horns. If cold, absorber-style calibrators are needed for some observations, we will be forced to put the feedhorns completely inside the cryostat. This has a large impact on the design of the cryostat, so we must choose carefully. However, we must also avoid including the calibrators "just in case" because they increase the complexity of the receiver significantly. The cold calibrators are not needed for the CBI point source measurements. A design for the polarizer/orthomode junction will be required, and we must also decide if the 27–39 GHz bandwidth of the commercial magic tees is acceptable. There are many other choices to make, such as whether to difference orthogonal polarizations, and whether to include the 3rd stage amplifiers between the magic tees, but these have a fairly small impact on the design.

The detector readout is fairly straightforward, but there are many options. We must decide whether or not to difference the detector outputs in hardware. If a total power mode is required, we must read out each detector individually. We must also decide whether to do the phase switch demodulation in hardware, as described in Section IV, or in software. For software demodulation, the CPU would have to read 12 16-bit words every phase switch period. This is probably impractical with a 25 μs period, but changing to 100 μs would not significantly degrade the noise performance. For the CBI observations, we are interested in point sources with flux densities in the range a few x 100 μJy to a few x 10 mJy. The sensitivity of the GBT, with the proposed radiometer, is $\sim$ 0.5 mJy/$\sqrt{\text{Hz}}$ in a 4-GHz bandwidth channel, so we probably do not want to integrate for much less than $\sim$ 1 s. With a 1 s readout period, it would be possible to communicate with the digital demodulator/integrator via a serial interface, and in this case, we would not need a CPU in the receiver chassis. However, if we do include a CPU in the receiver, we have the option of putting all the monitoring, control and continuum data collection in a single computer. The possibilities for this part of the system are endless, and the best approach depends very much on what already exists for the GBT, and what is planned for new receivers.

References

[1] http://map.gsfc.nasa.gov/m_mm/ob_techradiometers.html

http://www.astro.princeton.edu/~brookes/html/technical_info.html

[2] Norrod, R. and Srikanth, S., 1996, A Summary of the GBT Optics Design, National Radio Astronomy Observatory GBT Memo 155

[3] Clarricoats, P.J.B. and Olver, A.D., 1984, Corrugated Horns for Microwave Antennas (London: Peregrinus) p. 108 & 153

[4] Horowitz, P. and Hill, W., 1989, The Art of Electronics (Cambridge: Cambridge University Press:) p. 447